Appl. Phys. B 64, 293–300 (1997)

Applied Physics B Lasers and Optics

Vacuum ultraviolet gain measurements in optically pumped $LiYF_4:Nd^{3+}$

J. S. Cashmore, S. M. Hooker*, C. E. Webb

Department of Atomic and Laser Physics, University of Oxford, The Clarendon Laboratory, Parks Road, Oxford, OX1 3PU, UK
(Fax + 44-1865/272400)

Received: 4 March 1996 / Revised version: 10 July 1996

Abstract. We present measurements of the net-induced gain on the $5d$–$4f$ transition at 186 nm in $LiYF_4:Nd^{3+}$ optically pumped by radiation from a molecular fluorine laser. It is found that for $LiYF_4:Nd^{3+}$, one of a series of potential continuously tunable VUV lasers, relatively strong excited-state absorption results in net-induced loss. The prospects for VUV laser operation being realised in other rare-earth-doped fluorides is discussed.

PACS: 42.55.Rz

The possibility of generating coherent vacuum ultraviolet (VUV) radiation from solid-state media was investigated by Yang and DeLuca in 1976 [1]. Broad VUV fluorescence and excitation bands were observed in fluoride hosts doped with Nd^{3+}, Er^{3+} and Tm^{3+}, corresponding to the $5d$–$4f$ transitions in the activator ion. Yang and DeLuca proposed that these rare-earth-doped fluorides could operate as powerful and widely tunable VUV lasers. Later, Waynant [2, 3] reported observation of VUV laser oscillation at 172 nm on the $4f^2 5d$–$4f^3$ transition in a crystal of $LaF_3:Nd^{3+}$ optically pumped by Kr_2^* fluorescence at 146 nm, which was excited in turn by an electron beam. A number of rare-earth-doped fluoride systems operating in the VUV could be excited by radiation from a molecular fluorine laser [4, 5] which oscillates at 158 nm. Laser oscillation on the $5d$–$4f$ transition in $LaF_3:Nd^{3+}$, pumped by radiation from an F_2 laser, has been described [4, 6] and output pulse energies of 400 μJ and a maximum slope efficiency of 21% were reported.

In the light of these results, it is important to analyse other rare-earth-doped fluorides and to establish whether such systems exhibit optical gain at VUV wavelengths. In this paper, we present measurements of the transient gain on the $5d$–$4f$ transition in one of these potential VUV lasers, $LiYF_4:Nd^{3+}$, and interpret the results in terms of the kinetic processes involved in the optical pumping of rare-earth-doped fluorides. It is found that even after allowing for the passive absorption losses of the material in the excited region of the crystal, there is net *loss* for $LiYF_4:Nd^{3+}$. A possible explanation for this behaviour and the implications for VUV laser operation being realised in other rare-earth-doped fluorides are discussed.

1 Method for measurement of the net-induced gain

The simplest technique for measuring the gain in a prospective laser is to determine the amplification of a probe laser that is temporally and spatially coincident with the excited region of the material. However, there are very few suitable probe lasers in the VUV region of the spectrum and, therefore, an alternative method which indirectly measures the gain is described here. This method is based upon the measurement of the energy of amplified spontaneous emission (ASE) as a function of the length of the $LiYF_4:Nd^{3+}$ crystal excited by the optical pumping. This approach is similar to that described by Shaklee and Leheny [7] for the measurement of optical gain in semiconductor crystals in which the excited length of the sample was determined by the width of an adjustable slit positioned in the path of the pump beam. In the present case, the effect of the non-uniform energy distribution in the excitation beam of the F_2 laser and the induced passive absorption in the pumped region of the crystal is also considered in determining the net-induced gain (or loss).

The ASE signal $S(l)$ as a function of length l of the crystal which is excited by the F_2 laser is given by

$$S(l) = D_1 \int_0^l N_2(x)\,\Omega(x)\,\exp\left\{\int_0^x (\alpha(x') - k_0)\,\mathrm{d}x'\right\}\mathrm{d}x, \qquad (1)$$

where D_1 is a constant, $\Omega(x)$ is the solid angle subtended at a point x along the crystal by the limiting aperture of the detection system, k_0 the passive absorption coefficient in the pumped region of the crystal at the wavelength of the $5d$–$4f$ transition, and $N_2(x)$ and $\alpha(x)$ are the upper-level

* Presently at Edward L. Ginzton Laboratory, Stanford University, Stanford, CA 94301, USA

population density and the net small-signal gain coefficient induced at x by the optical pumping.

In order to determine the magnitude of $\alpha(x)$ from the measured behaviour of the ASE signal in the case of non-uniform pumping, it is necessary to know the dependence of $N_2(x)$ and $\alpha(x)$ with the position x along the crystal. As described below, the variation of the fluence $F(x)$ of the pump laser with x is measured directly and, therefore, we require relations between $N_2(x)$ and $F(x)$ and between $\alpha(x)$ and $F(x)$. The variation of the peak upper-level population density N_2 with the pump fluence, and hence with x, is determined from measuring the energy of the spontaneous emission from a very short excited length of the crystal as a function of the pump fluence at that point. In practice, it was found that N_2 varied almost linearly with pump fluence and, therefore, it was assumed that $N_2(x) \propto F(x)$. A direct measurement of the dependence of $\alpha(x)$ with the fluence $F(x)$ cannot be made and therefore some assumption about this relationship is required. The simplest two assumptions are that either $\alpha(x)$ is proportional to $F(x)$ or that it is approximately constant with fluence. The consistency of the assumption may then be verified from the variation of the deduced values of the net-induced gain coefficient with the pump fluence. The measured ASE signal $S(l)$ is fitted to (1) to yield values for the multiplicative constant D_1, and a parameter which is equal to either the net-induced gain coefficient per unit pump fluence, or the (uniform) net-induced gain coefficient, depending upon the assumption as to the form of $\alpha(x)$. The approximations need only be valid over the range of pump fluences present in a given experiment as a result of the non-uniform energy distribution across the F_2 laser beam. The typical fractional variation about the average value measured in a pump fluence profile was $\pm$ 50%.

In the case of the rare-earth-doped fluorides, it is found that the passive absorption coefficient k_0 is frequently higher than that measured in the bulk of the crystal, due to the formation of long-lived colour centres by the optical pumping. The value of k_0 in the pumped region may be measured directly by a slight alteration in the experimental arrangement for the gain measurements. If a slit or pinhole of width Δx is scanned along the length of the crystal, consideration of the absorption of the spontaneous emission by the unirradiated region of the crystal gives the signal $\Delta S(x)$ recorded as a function of the position x of the pinhole as

$$\Delta S(x) = D_2 F(x)\, \mathrm{e}^{-k_0 x}\, \Delta x, \tag{2}$$

where D_2 is a constant, k_0 is the passive absorption coefficient in the pumped region of the crystal, and it has been assumed that $N_2(x) \propto F(x)$.

2 Gain measurement

2.1 Experimental arrangement for the gain measurement

The apparatus used to determine the net-induced gain is shown schematically in Fig. 1. The pump laser was a small discharge excited F_2 laser, which has been described in

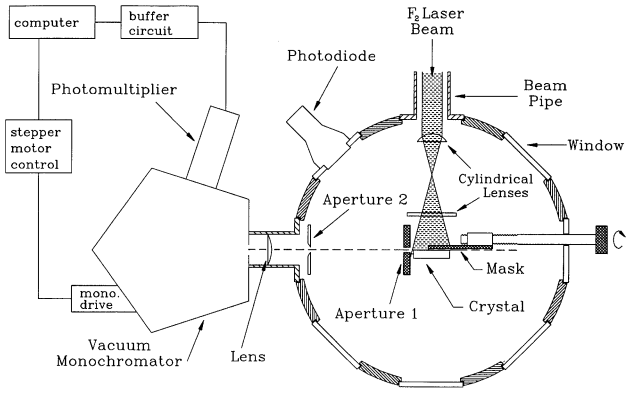

Fig. 1. Schematic diagram of the experimental arrangement used to determine the net-induced gain in $LiYF_4:Nd^{3+}$

detail elsewhere [8]. In the present experiments, it was typically operated with a gas mixture comprising 6 mbar of fluorine in a helium buffer gas at a pressure between 1.5 and 3.5 bar. The output energy of the F_2 laser could be varied between 2 and 42 mJ per pulse by adjusting the helium buffer gas pressure and the charging voltage of the external capacitor. The laser was operated at a pulse repetition frequency of 0.3 Hz throughout all the experiments.

The $LiYF_4:Nd^{3+}$ crystal was grown under a reactive atmosphere using the Czochralski technique, and finished as an optically polished cylindrical rod of diameter 5 mm and length 30 mm. A polished plane pump face 3 mm high ran along the length of the rod. The concentration of the Nd^{3+} dopant was approximately 0.4 mol% and the c-axis of the crystal was orientated along the axis of the cylinder.

Radiation from the F_2 laser was focused onto the crystal by a crossed pair of plano-convex magnesium fluoride cylindrical lenses, both of focal length 30 mm. The lenses were arranged such that the height of the F_2 laser beam at the pump face of the crystal was approximately 2 mm and its width at the pump face, in the direction of the axis of the crystal, was about 35 mm.

The length l of the pump face of the crystal exposed to the F_2 laser radiation was controlled by the position of a metal mask, as shown in Fig. 1. Its position was altered by rotation of a threaded rod that passed through a threaded block, which was attached to the mask. The block was free to slide, but not to rotate, in a "U"-shaped holder. In this way, the mask could be linearly translated across the face of the crystal whilst the experiment chamber was evacuated. The distance moved by the mask was determined by the 1.5 mm pitch of the thread.

Amplified spontaneous emission from the crystal passed through two apertures before being focused by a calcium fluoride lens of 100 mm focal length onto the entrance slit of a 0.2 m VUV monochromator (GCA/McPherson 234). The monochromator was set to a wavelength of 186.2 nm which was measured to be the peak of the $LiYF_4:Nd^{3+}$ $5d$–$4f$ fluorescence band. The entrance slit of the monochromator was 700 μm wide, corresponding to a bandwidth of 2.6 nm. The two apertures controlled the solid angle of collection, and the volume from which radiation was detected. The first

aperture defined the volume from which the ASE could be detected, and comprised a circular hole of 400 μm diameter, positioned approximately 1 mm from the end of the crystal nearest to the monochromator. The second aperture, positioned 180 mm from the end of the crystal, defined the solid angle of collection of the detection system and comprised a 1 mm high adjustable slit, set to 500 μm width in the direction of the F_2 laser beam. The region sampled was therefore essentially cylindrical with a diameter of 400 μm and a length equal to that of the crystal. The axis of the cylinder was approximately 200 μm from the crystal pump face.

The pump fluence at the face of the crystal decayed slowly throughout the course of each gain or absorption measurement due to both a decrease in the F_2 laser pulse energy and the deposition of an absorptive layer of vacuum pump oil at the surfaces of the magnesium fluoride lenses. A vacuum photodiode (ITL 1850 S20) was used to monitor the pump fluence reaching the crystal from a measurement of the energy of the F_2 laser radiation scattered from the metal mask. The pump fluence at the crystal decayed approximately linearly with the number of F_2 laser pulses, and hence the reduction of the pump fluence with x during a gain or k_0 measurement was obtained by multiplying the measured $F(x)$ by a linear term of the form $(1 - \beta x)$. Typically, the pump fluence decreased by 20–30% over the course of an experimental run depending on the total number of F_2 laser pulses and the initial pulse energy. The magnitude of the decay coefficient β was found to be typically $5\text{–}10 \times 10^{-3}\ \text{mm}^{-1}$.

The radiation transmitted by the monochromator was detected by a UV/VUV photomultiplier (EMI 9426B) and its output was integrated and then passed to a personal computer. The firing of the F_2 laser, the wavelength setting of the monochromator and the acquisition of the integrated signal were all controlled by the same computer. Typically, 16 pulses of the pump laser were averaged for each data point.

The variation of the peak upper-level population density N_2 induced by the optical pumping was determined by positioning the metal mask so as to irradiate with F_2 laser radiation only approximately 1 mm at the end of the crystal nearest to the detector. The spontaneous emission signal was measured as a function of the pump fluence at that point.

In order to measure the passive absorption coefficient k_0, the metal mask was simply replaced by a 1 mm wide slit which was then scanned along the pump face of the crystal, whilst the F_2 laser was fired and the spontaneous emission signal was recorded as before. It is important to note that at each pump fluence datum, the gain or k_0 measurements were performed without disturbing the alignment of the apparatus. As a result, any initial small misalignment of the apertures or crystal would not have affected the net-induced gain determined by this method.

The fluence distribution of the F_2 laser radiation across the pump face of the crystal was recorded by replacing the metal mask with a joulemeter (Gentec ED-100A) and scanning the detector in the plane corresponding to the crystal pump face after the sample had been removed from the chamber. The active surface of the joulemeter was apertured by a circular hole of 1 mm diameter and the pump fluence was measured over this area. A unity-normalised quartic expression for the fluence distribution $F(x)$ was fitted to the observed variation of the pump fluence with the position x.

2.2 Results of the gain measurement

Figure 2 shows the measured ASE signal as a function of the length of the crystal exposed to the F_2 laser radiation for an average pump fluence along the length of the crystal of $10.0\ \text{mJ cm}^{-2}$. The signal increases approximately linearly with length for small x and then rolls over and is approximately constant for the last 10 mm length of the crystal. Also shown is a fit of the data to the ASE signal given in (1) and a fit to the fluorescence signal also given in (1) with both the gain coefficient $\alpha(x)$ and the passive absorption coefficient k_0 set equal to zero. For both fits, the decay of the pump fluence defined by the decay coefficient β was taken into account. A comparison of the two fits shows that the roll-off in the measured data is not the result of the non-uniform pumping, but is due to the net loss in the crystal at the wavelength of the fluorescence.

Figure 3 shows a typical result of a measurement of the passive absorption coefficient k_0 at the same average pump fluence as in Fig. 2 and a fit to (2). The absorption coefficient was found to increase monotonically with the fluence of the F_2 laser from 0.3 to $1.3\ \text{cm}^{-1}$ over the fluence range of 1–42 mJ cm^{-2}. For comparison, the absorption coefficient in the bulk of the crystal was measured by a combination of a D_2 lamp and a vacuum monochromator to be only $0.08\ \text{cm}^{-1}$ at a wavelength of 186.2 nm. Due to the progressive increase in the passive absorption, the gain measurements were performed with progressively increasing pump fluences. The crystal was exposed to each pump fluence for approximately 30 pulses prior to a measurement which ensured that the value of k_0 did not change later during the gain measurement itself.

The increase in the passive absorption of the optically pumped region with increasing F_2 laser fluence was

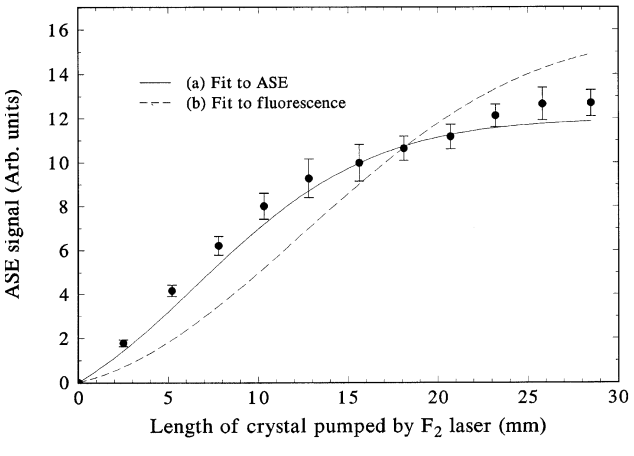

Fig. 2. The measured variation of the amplified spontaneous emission signal as a function of the length of crystal pumped by the F_2 laser at a volume-averaged fluence of $10.0\ \text{mJ cm}^{-2}$. Also shown are: (a) a fit to the ASE signal in (1), and (b) a fit to the fluorescence signal also given by (1) but with $\alpha(x)$ and k_0 set equal to zero

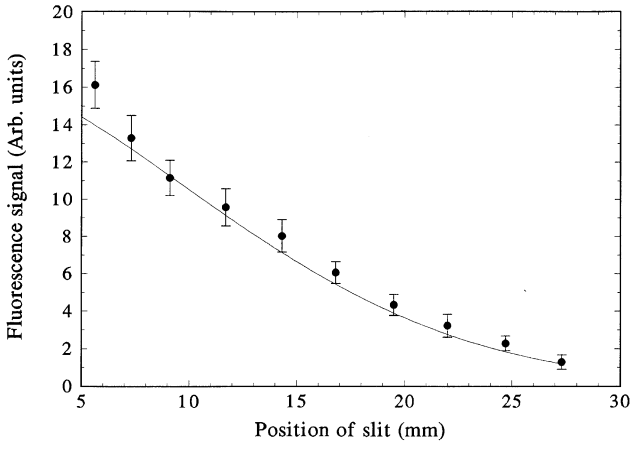

Fig. 3. Typical measurement of the passive absorption coefficient k_0, together with a fit to (2). The volume-averaged fluence of the pump laser was 10.0 mJ cm^{-2}

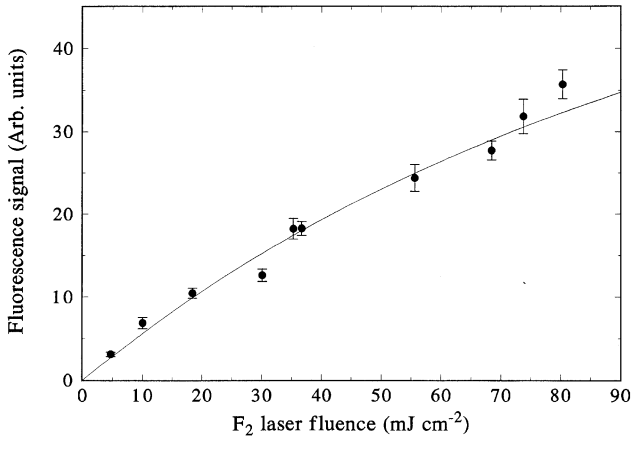

Fig. 4. The measured variation of the laser-induced fluorescence signal as a function of the fluence of the pump laser. Also shown is a fit to (A3)

almost certainly due to the creation of long-lived colour centres in the sample. It was observed that the pumped region developed a distinct brown coloration after exposure to the pump radiation. This coloration could be removed by irradiating the crystal to low-intensity UV radiation from a Hg lamp for 4–6 h or by heating to 75 °C for a period of approximately 12 h.

The peak upper-level population density was found to increase almost linearly with pump fluence over the range 5–80 mJ cm^{-2}, as shown in Fig. 4. Figure 5 shows the calculated net-induced small-signal gain coefficient as a function of the average pump fluence along the length of the crystal where it has been assumed that both the upper-level population density and the net-induced gain coefficient vary linearly with the pump fluence. The behaviour of the calculated gain coefficient is observed to be approximately consistent with the latter assumption. It is also evident that the net-induced gain coefficient is negative and decreases monotonically with increasing pump fluence.

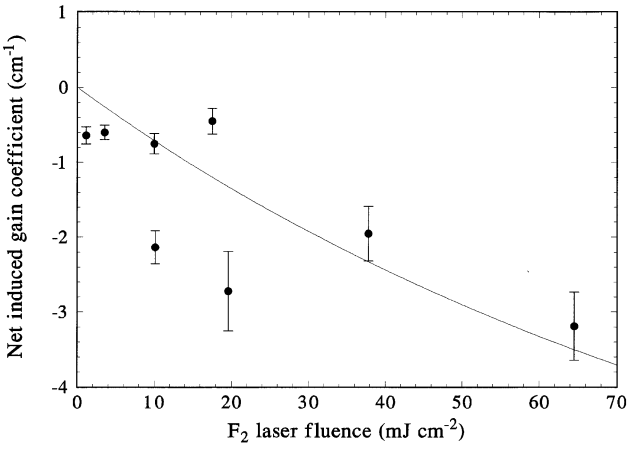

Fig. 5. The measured net-induced gain coefficient as a function of the volume-averaged pump fluence, together with a fit to (3)

3 Observe transient absorption

3.1 Experiments to observe transient absorption

The kinetic model presented in the appendix describes the significant processes involved in the optical pumping of the rare-earth-doped fluorides, and in particular the absorption of the 5*d*–4*f* radiation by transient colour centres created by the pump laser radiation. An experiment to observe the transient absorption directly was carried out in an attempt to verify this process and to compare the results with the kinetic model. A conventional pump-probe technique was employed for this measurement and the transient reduction in the intensity of the probe beam transmitted through the pumped region of the crystal was recorded.

The experimental arrangement was similar to the gain measurements except that the two apertures were removed. The unpolarised beam from a helium–neon laser at a wavelength of 633 nm was focused by a quartz lens of focal length 450 mm to a spot of approximately 0.5 mm in diameter at the end face of the crystal. The probe beam passed through the region of the crystal excited by the F_2 laser such that the whole of the He–Ne beam lay just inside the crystal pump face. After traversing the crystal, the He–Ne laser radiation passed through an interference filter with a peak transmission bandwidth of 1.2 nm centred at 632.8 nm. The transmitted probe beam was detected with a fast photomultiplier (Burle IP28) and the output signal was recorded by a 500 MHz digital oscilloscope (Hewlett-Packard HP54111D). The temporal profile of the F_2 laser pulse was measured by a vacuum photodiode (ITL 1850 S20) which detected the pump laser radiation scattered from the first cylindrical focusing lens. The rise time of the photodiode was approximately 100 ps and the rise time of the detection system for the probe laser radiation was estimated to be 2 ns.

3.2 Results of experiments to observe transient absorption

The intensity of the helium–neon laser radiation transmitted by the $LiYF_4:Nd^{3+}$ crystal as a function of time

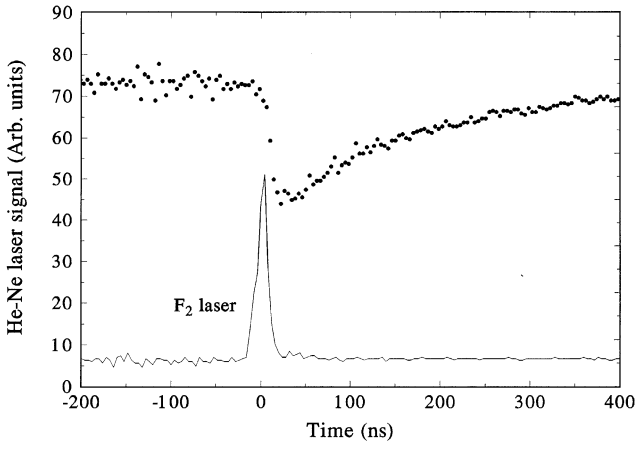

Fig. 6. Temporal evolution of the transmitted intensity of the helium–neon laser relative to the F_2 laser pulse for a volume-averaged pump fluence of 65 mJ cm^{-2}

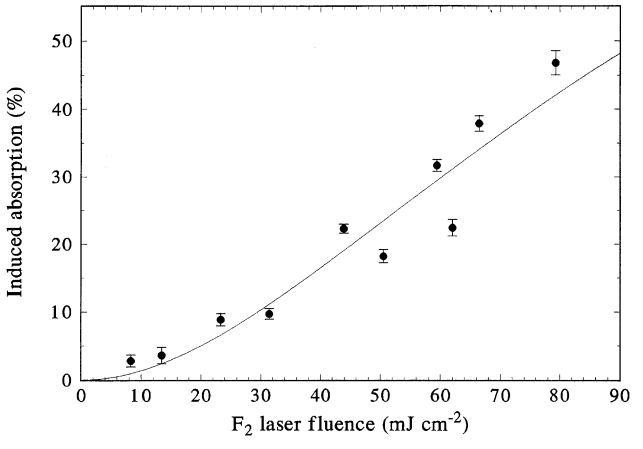

Fig. 7. The measured induced absorption at the wavelength of the helium–neon laser as a function of the volume-averaged fluence of the F_2 laser, together with a fit to (A5)

during the F_2 laser pump pulse is shown in Fig. 6 for an average pump fluence along the length of the crystal of approximately 65 mJ cm^{-2}. A pronounced absorption, with a rise time corresponding to the duration of the pump laser pulse and a decay period of several hundred nanoseconds is apparent. The observed absorption is almost certainly due to the formation of transient colour centres by the optical pumping. Heating of the crystal by the pump pulse has a negligible effect upon the transient absorption since calculations indicate that thermal lensing is weak and any induced lens is expected to decay with a thermal time constant of between 0.1 and 3 s which is much longer than the lifetime of the observed transient absorption. Other processes, such as a transition from the lowest 5*d* level of the Nd^{3+} ion to a higher lying 5*d* state can be excluded since the lifetime measured is much longer than would be expected for such a transition. In Fig. 7 the induced absorption of the He–Ne laser radiation is plotted as a function of the average pump fluence along the length of the crystal. The induced absorption is seen initially to rise quadratically with the pump fluence which reflects the two-step excitation of the transient colour centres. Also shown in Fig. 7 is a fit to the data of the expression (A5) derived in the appendix for the number density of transient colour centres at the end of the pump pulse.

4 Analysis of the results

The results of the measurements of the gain and the induced absorption were analysed in terms of the kinetic model derived in the appendix as follows. The fit to (A3), shown in Fig. 4, of the observed variation of the peak upper-level population density N_2 with the pump fluence measured at the pump face of the crystal yielded a value of the photoionisation cross-section σ_{2I} from the $Nd^{3+}5d$ level at the wavelength of the F_2 laser. The variation of the fluence into the crystal over the pumped region was not precisely known since this depended upon the absorption length of the F_2 laser radiation in the crystal. The absorption length was estimated to be 0.3 mm which is comparable with the depth of the region of the crystal from which the fluorescence was collected (200 μm behind the pump face). However, the absorption length is uncertain to $\pm$ 50% and therefore in this analysis the fluence measured at the pump face of the crystal was used as an approximation for the volume-averaged fluence at the sampled region. The error in the values of the cross-sections derived with this assumption for the fluence is significantly less than the overall error on the cross-sections given below which is directly related to the uncertainty in the absorption length of the pump radiation. Given the value for σ_{2I}, the fit to (A5) of the measured variation of the induced transient absorption at 632.8 nm with pump fluence, yielded a value for the cross-section for bleaching of the induced colour centres σ_B at the F_2 laser wavelength. This fit, shown in Fig. 7, is seen to agree well with the measured data. The results of the fits are:

$$\sigma_{2I} = 15.9 \pm 6.2 \times 10^{-18}\ \text{cm}^2; \quad \sigma_B = 12.2 \pm 5.3 \times 10^{-18}\ \text{cm}^2.$$

Having deduced values for the cross-sections σ_{2I} and σ_B, together with their estimated errors, an attempt was made to fit the expression given in (A7) to the measured variation of the net-induced small-signal gain coefficient with the pump fluence. This procedure determined values for the net gain cross-section σ_{21}^{net} at 186.2 nm and a parameter $\eta\sigma_c$ equal to the product of the probability η of a photoionisation event resulting in the production of a transient colour centre and the cross-section σ_c for absorption of the 5*d*–4*f* fluorescence by the induced colour centre. Although this analysis reproduced the measured data reasonably well, no reliable value for the parameter $\eta\sigma_c$ could be obtained since, as discussed below, the induced loss was dominated by excited-state absorption and the absorption due to transient colour centres was small by comparison. The kinetic model was modified so that the absorption due to the induced colour centres was neglected. Equation (A7) was therefore replaced by

$$\alpha = \sigma_{21}^{net} N_2(\tau_p), \tag{3}$$

where $N_2(\tau_p)$ is the population density of the upper level at the end of the F_2 laser pulse given in (A3). From the fit of this expression to the measured variation of the net-induced gain coefficient with the average pump fluence shown in Fig. 5 it is seen that (3) agrees well with the experimental data. The resulting value for the net gain cross-section is

$$\sigma_{21}^{net} = -4.2 \pm 2.1 \times 10^{-18}\ \text{cm}^2.$$

5 Discussion

Despite the fact that the passive absorption in the excited region of the crystal, including the creation of long-lived colour centres, was considered in the analysis, the induced optical gain was found to be negative and to become more negative with increasing pump fluences. The population density of the lowest Nd^{3+} 5*d* level was found to increase almost linearly with the F_2 laser fluence and therefore the net induced loss strongly suggests a significant absorption at 186.2 nm as a direct consequence of the optical pumping. There are two possible causes of the absorption of the 5*d*–4*f* fluorescence in the crystal: the first is excited-state absorption (ESA) by Nd^{3+} ions in the 5*d* level terminating in the conduction band, and the second is absorption due to transient colour centres created by the F_2 laser radiation. The formation of colour centres which are absorptive at the wavelength of a helium–neon laser was observed directly. However, the fact that the measured net-induced gain coefficient is negative at very low pump fluences implies that ESA dominates the induced absorption, since the number density of induced colour centres during the pump pulse is very small at low pump fluences. Indeed, as mentioned above, the absorption of the 5*d*–4*f* fluorescence by transient colour centres was too small to be determined from a fit to the measured net gain coefficient.

We may estimate the gain cross-section of the 5*d*–4*f* transition in $LiYF_4:Nd^{3+}$ by assuming that the transition at 186.2 nm has a Lorentzian line shape with a full-width at half-maximum of approximately 8.3 nm. This line width was obtained from the F_2 laser-induced fluorescence spectrum of the 0.4% $LiYF_4:Nd^{3+}$ crystal recorded with the VUV monochromator. From the spectrum we estimate the VUV fluorescence quantum yield to be 60%. Together with the fluorescence lifetime of the upper level, this gives a value for the gain cross-section σ_{21} of the 5*d*–4*f* transition of approximately $2.2 \times 10^{-18}\ \text{cm}^2$. The cross-section for excited state absorption σ_{ESA}, at a wavelength of 186.2 nm, is obtained from the difference of the transition gain cross-section σ_{21} and the observed net gain cross-section σ_{21}^{net} and has a value of $\sigma_{ESA} = 6.4 \pm 2.1 \times 10^{-18}\ \text{cm}^2$.

Both the excited-state absorption of the fluorescence radiation, characterised by σ_{ESA}, and the mechanism for colour centre formation, determined by σ_{2I}, involve photoionisation of Nd^{3+} ions in the 5*d* level to the conduction band. The values for the cross-sections σ_{ESA} and σ_{2I} determined in the present work are in very good agreement with measured photoionisation cross-sections from the 5*d* level to the conduction band found for rare-earth ions in insulators and semiconductors [9, 10]. For example, Hamilton et al. [11] measured the photoionisation cross-section of the 5*d* level in $Y_3Al_5O_{13}:Ce^{3+}$ as a function of wavelength and found the peak value of the cross-section was $(10 \pm 3) \times 10^{-18}\ \text{cm}^2$ at a wavelength of 700 nm with a full-width at half-maximum of approximately 0.6 eV. The factor of three between the magnitudes of the cross-sections σ_{ESA} and σ_{2I} measured above is due to the different wavelengths of the fluorescence and pump laser and is consistent with a photoionisation cross-section width of order 1 eV.

We have observed the formation of both long- and short-lived colour centres, and successfully modelled their formation in terms of photoionisation of Nd^{3+} ions in the 5*d* level by the optical pumping. The formation of colour centres by this mechanism has been reported in $Y_3Al_5O_{13}:Ce^{3+}$ [11], $CaF_2:Ce^{3+}$ [12], and $LiYF_4:Ce^{3+}$ [13].

6 Conclusions

A *negative* net-induced gain coefficient has been measured on the VUV 5*d*–4*f* transition of $LiYF_4:Nd^{3+}$ following optical excitation with F_2 laser radiation. The loss is present even at very low values of the pump fluence and, therefore, even in the absence of other loss processes this transition cannot show laser oscillation in $LiYF_4:Nd^{3+}$. A kinetic model of the optical pumping processes in rare-earth-doped fluorides was developed which reproduces the observed behaviour of the net-induced loss as a function of the pump fluence.

The negative gain coefficient measured for $LiYF_4:Nd^{3+}$ arises from the fundamental fact that the cross-section for ESA exceeds the gain cross-section of the 5*d*–4*f* transition. This intrinsic problem is likely to be important for other rare-earth-doped fluorides since the peak cross-section for ESA to the conduction band is expected to be of the order $1 \times 10^{-17}\ \text{cm}^2$ with a bandwidth of order 1 eV, compared to the predicted gain cross-section of approximately $2 \times 10^{-18}\ \text{cm}^2$. The position of the peak of the ESA spectrum relative to that of the 5*d*–4*f* fluorescence in a particular dopant ion–host lattice combination is therefore crucial to determining whether optical pumping will induce net gain or loss. Direct measurements of the onset of photoconductivity and the ESA cross-section in the VUV spectral region for the rare-earth-doped fluorides would be useful in deciding whether a change in the dopant–host combination could reduce the ESA cross-section below the gain cross-section at the prospective laser wavelength.

Even if the ESA cross-section were reduced below the gain cross-section, laser oscillation might still be prevented due to the formation of colour centres induced by the optical pumping. For example, in the present case the predicted gain cross-section and (A3) lead to a gain coefficient of $1.3\ \text{cm}^{-1}$ at a pump fluence of $42\ \text{mJ cm}^{-2}$, in the absence of ESA. This compares with the passive absorption coefficient in the pumped region of the crystal due to the long-lived colour centres which was measured to be $1.3\ \text{cm}^{-1}$. The creation of transient colour centres during the pump pulse would reduce the net gain still further. It is interesting to note that in similar measurements to those

reported here on several crystals of $LaF_3:Nd^{3+}$ available to us, we have obtained similar results, i.e. optical pumping of the crystals induces net loss at the wavelength of the VUV 5*d*–4*f* transition in $LaF_3:Nd^{3+}$. In this case, the loss is almost certainly due to colour centres induced by the short wavelength pumping. We have measured large passive absorption losses due to long-lived colour centres created in $LaF_3:Nd^{3+}$ following excitation with F_2 laser radiation even at low pump fluences. There remain many obstacles to overcome before the rare-earth-doped fluorides can achieve their potential as sources of tunable VUV laser radiation.

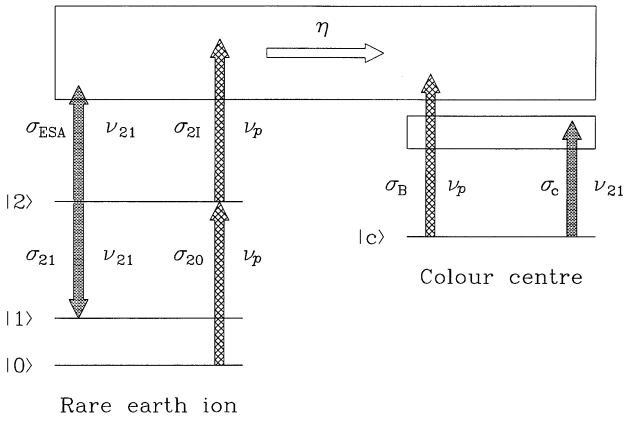

Fig. 8. Schematic diagram of the population transfer processes included in the kinetic model of the optical pumping of the rare-earth-doped fluorides

Appendix A

Rate equation model for the optical pumping of rare-earth-doped fluorides

This appendix details the kinetic model used to describe the processes which occur when the rare-earth-doped fluorides are optically pumped. This model is similar to that discussed by Pogatshnik and Hamilton [8] for the creation of colour centres in $CaF_2:Ce^{3+}$ in which the build up of a steady state of long-lived colour centres as a function of the number of applied pump pulses was considered. In this treatment, the evolution of the net-induced gain during a single pump pulse is modelled. The essential features of the optical pumping processes are shown schematically in Fig. 8.

Ions in the ground state $|0\rangle$ are excited to the upper laser level $|2\rangle$ by absorption of pump laser radiation of frequency ν_p (neglecting the phonon-assisted relaxation to the lowest 5*d* level). Excited-state absorption of the pump laser radiation at the upper level $|2\rangle$ terminates in the conduction band of the host. A probability η is then assigned for each ESA event to the formation of a colour centre which is absorptive at the fluorescence frequency ν_{21} and is created by the trapping of the electron at a crystal defect. The lifetime of these colour centres is assumed to be long compared to the duration of the pump pulse. Photobleaching of the colour centres at the frequency of the pump radiation is assumed to take place with a cross-section σ_B. The model assumes that population transfer by absorption or stimulated emission of fluorescence from level $|2\rangle$ is negligible compared with the other transfer processes. This approach includes the essential processes required to determine the population of the upper level $|2\rangle$ and is therefore a reasonable approximation for the population inversion. The approximation is valid whilst the gain is small enough that significant population is not transferred from level $|2\rangle$ which was found to be true in the present case.

With the approximation of the pump pulse as a square pulse of duration τ_p and fluence F_p, the population density N_2 of the upper level of the rare earth ion is given by the rate equation

$$\frac{dN_2}{dt} = \frac{\sigma_{20}F_p}{h\nu_p\tau_p}N_0 - \frac{\sigma_{2I}F_p}{h\nu_p\tau_p}N_2 - \frac{N_2}{\tau_2}, \tag{A1}$$

where τ_2 is the radiative lifetime of the upper level, σ_{20} and σ_{2I} are the optical cross-sections for the pump transition and photoionisation of the 5*d* level. The density of colour centres N_c is similarly given by

$$\frac{dN_c}{dt} = \eta\frac{\sigma_{2I}F_p}{h\nu_p\tau_p}N_2 - \frac{\sigma_B F_p}{h\nu_p\tau_p}N_c, \tag{A2}$$

where σ_B is the cross-section for bleaching of the induced colour centres by the pump laser radiation. The intensity of the optical pumping is assumed to be well below the saturation intensity of the pump transition from state $|0\rangle$ to state $|2\rangle$ and, therefore, the depletion of the ground state is considered negligible. The peak values of N_2 deduced from the fits to the measured data were always found to be small (less than 1%) compared to the ground-state population density N_0, consistent with this assumption.

The boundary conditions that the population density of the upper level and the density of the colour centres are both zero at the start of the pump pulse yield solutions for N_2 and N_c at the end of the pump pulse as

$$N_2(\tau_p) = N_0\sigma_{20}\frac{F_p\tau_2'}{h\nu_p\tau_p}\left\{1 - \exp\left(\frac{-\tau_p}{\tau_2'}\right)\right\}, \tag{A3}$$

where

$$\frac{1}{\tau_2'} = \frac{1}{\tau_2} + \frac{\sigma_{2I}F_p}{h\nu_p\tau_p} \tag{A4}$$

and

$$N_c(\tau_p) = \eta N_0\sigma_{20}\sigma_{2I}\frac{F_p^2\tau_2'\tau_c'}{(h\nu_p\tau_p)^2} \times \left\{1 - \exp\left(\frac{-\tau_p}{\tau_c'}\right) - \frac{\tau_2'}{\tau_2' - \tau_c'} \times \left[\exp\left(\frac{-\tau_p}{\tau_2'}\right) - \exp\left(\frac{-\tau_p}{\tau_c'}\right)\right]\right\}, \tag{A5}$$

where

$$\frac{1}{\tau_c'} = \frac{\sigma_B F_p}{h\nu_p\tau_p}. \tag{A6}$$

Table A1. Values of the known parameters used in the kinetic model

Parameter	Value	Error	Comment
$(N_0\sigma_{20})^{-1}$	0.3 mm	$\pm$ 0.15 mm	Observed absorption depth of pump radiation
τ_p	30 ns	$\pm$ 5 ns	Measured
τ_2	35 ns	$\pm$ 5 ns	Measured

The net-induced gain coefficient immediately after the pump pulse is then given by

$$\alpha = \sigma_{21}^{\text{net}} N_2(\tau_p) - \sigma_c N_c(\tau_p), \tag{A7}$$

where

$$\sigma_{21}^{\text{net}} = \sigma_{21} - \sigma_{\text{ESA}}, \tag{A8}$$

in which σ_{21} is the gain cross-section of the laser transition and σ_c is the absorption cross-section of the induced colour centres at the $5d$–$4f$ fluorescence wavelength, and σ_{ESA} is the cross-section for excited-state absorption at the same wavelength.

The known parameters of the model were assigned the values given in Table 1. Note that the observed absorption depth of the pump radiation in the $LiYF_4:Nd^{3+}$ crystal corresponds to the parameter $(N_0\sigma_{20})^{-1}$.

Acknowledgements. We would like to acknowledge many useful discussions on optically pumped rare-earth-doped fluoride lasers with M.A. Dubinskii, formerly of Kazan State University, and A.C. Cefalas of the National Hellenic Research Foundation, Athens. We are very grateful to A. Egesel and R.C.C. Ward for considerable care in the preparation of the crystal sample. This work was performed as part of a collaborative programme of research funded by the European Union through contract number ERB-SCI-CT92-0794. One of us (SMH) is grateful to the EPSRC for funding via grant number GR/H72885, and JSC appreciates the support of an EPSRC studentship.

References

1. K.H. Yang, J.A. DeLuca: Appl. Phys. Lett. **29**, 499 (1976)
2. R.W. Waynant: Appl. Phys. B **28**, 205 (1982)
3. R.W. Waynant, P.H. Klein: Appl. Phys. Lett. **46**, 14 (1985)
4. M.A. Dubinskii, A.C. Cefalas, C.A. Nicolaides: Opt. Commun. **88**, 122 (1992)
5. S.M. Hooker, C.E. Webb: Prog. Quantum Electron. **18**, 227 (1994)
6. M.A. Dubinskii, A.C. Cefalas, E. Sarantopoulou, S.M. Spyrou, C.A. Nicolaides, R.Yu. Abdulsabirov, S.L. Korableva, V.V. Semashko: J. Opt. Soc. Am. B **9**, 1148 (1992)
7. Shaklee, Leheny: Appl. Phys. Lett. **18**, 475 (1971)
8. S.M. Hooker, C.E. Webb: IEEE J. Quantum Electron. **26**, 1529 (1990)
9. D.S. Hamilton: In *Tunable Solid State Lasers* (Springer, Berlin 1985) pp. 80–90
10. J.K. Lawson, S.A. Payne: Phys. Rev. B **47**, 14003 (1993)
11. D.S. Hamilton, S.K. Gayen, G.J. Pogatshnik, R.D. Ghen: Phys. Rev. B **39**, 8807 (1989)
12. G.J. Pogatshnik, D.S. Hamilton: Phys. Rev. B **36**, 8251 (1987)
13. K.-S. Lim, D.S. Hamilton: J. Opt. Soc. Am. B **6**, 1401 (1989)